Tenth International Conference on Computational Fluid Dynamics (ICCFD10), Barcelona,Spain, July 9-13, 2018

ICCFD10-2018-xxxx

Numerical Simulation of the Noise from a Supersonic Hot Jet with High Order Finite Difference Scheme

J.H. Gao*[a], X.D. Li*
Corresponding author: gaojhui@buaa.edu.cn

* School of Energy and Power Engineering, Beihang University, Beijing, China.
[a]Collaborative Innovation Center for Advanced Aero-Engine.

Abstract: In this study the screech tones from a supersonic hot jet is simulated with a high order computational aeroacoustic solver. The 4th order Dispersion Relation Preserving (DRP) scheme [25] is used for spatial discretization. The grid block interface flux reconstruction method (IFR) for high order finite difference scheme proposed by the present authors is utilized [26, 27] to handle the flux on the block interface. The Low-Dissipation & Low-Dispersion Runge-Kutta scheme [28] in the 2N storage form is employed for time integration. To eliminate the grid spurious oscillations, a high order explicit spatial filter is applied at each time step. An adaptive shock capturing method based on the variable stencil Reynolds number method of Tam & Shen [29] is adopted to capture the shock cells in the jet plumes, but has little influence on the other components in the flow field. Proper non-reflective boundary conditions are applied to the far-filed and outflow boundary regions. The simulation is conducted for the jet in the Mach number range from 1.2 to 1.56 at four reservoir temperature ratios (Tr/T_∞), which are 1.0, 1.67, 2.32 and 2.78 respectively. The pressure field and shock-cell structures of the screeching jet are presented. The near field noise spectra are presented and analyzed. The computed frequencies and amplitudes of the screech tones from the cold jet are compared with the experimental data by Ponton et. al. [22], and a good agreement is obtained. The effects of the jet temperature on the screech tones are studied. It is found that the frequencies of the screech tones increase with the jet temperature, but the amplitudes decreases slightly with the temperature.

Keywords: Supersonic Hot Jet, Computational Aeroacoustics, Screech Tones, Temperature Effect.

1 Introduction

Jet screech has long been a fascinating subject of aeroacoustic research since Powell's first observation [1] in 1951. A large number literatures have been published for understanding, prediction and controlling of the complex nonlinear feedback phenomena. Among various investigations, experiments have played key roles for understanding screech generation mechanism and constructing theoretical models [2]. The pioneering experimental observation of Powell elucidated jet screech as a nonlinear feedback loop mechanism and thus based for the construction of his monopoles model [1]. The following twenty years experimental investigations have been concerned for the understanding of more detailed process of screech generation, such as the works by Merle [3], Davies & Oldfield [4], Westley & Wooley [5] and Poldervaart [6]. Chan [7] then proposed a dipole model for the prediction of jet screech. In 1980's and 1990's, NASA Langley and Glenn Research Centers investigated jet screech phenomena by more refined experimental techniques and detailed measurements. Very rich databases have been obtained for understanding jet screech and validating theoretical models. For example, Ponton & Seiner [8] studied the effects of nozzle exit lip thickness at a wide range of Mach number, and obtained a detailed database of the screech frequencies and amplitudes. Panda [9, 10] investigated the screech generating process and provided the dynamic cycles of shock motions. In this period, several theoretical models were proposed, such as the multiple-scales shock-cell model by Tam [11], the linear shock-

cell model by Morris [12] and the waveguide theory by Tam [13]. Most of the experimental studies concerned the cold jet, except Massey et al. [14, 15, 16]. They measured the screech tones from hot jets in the anechoic and semi-anechoic chambers, and studied the effect of temperature on the screech tones. It was found that the amplitudes of the screech tones varied slightly or even increased with the jet temperature. Although Massey et al. measured the frequencies and amplitudes of the hot screeching jets in detail, their data were ambiguous because most of their experiments were conducted in a semi-anechoic chamber. The reflection of the ground would have effects on the screech tones.

During the past twenty years, numerical simulations of screech have advanced significantly. Shen & Tam [17] obtained excellent results in a numerical simulation of axisymmetric screech for circular jets with $k-\epsilon$ turbulence model. They extended their work to three-dimension (3D) [18] by expanding the solution by Fourier series in the azimuthal direction. Shen & Tam [19] also studied the effects of jet temperature and nozzle lip thickness on screech tones. However, they only compared the frequencies with the experimental data of Massey et al. [14]. The effect of temperature on the amplitudes of screech tones is still unknown. Li and Gao [20, 21] simulated the axisymmetric and three-dimensional round supersonic screeching jet with a CAA method. Their calculated screech tone wavelengths and amplitudes over a wide range of Mach number agree well with the experimental data of Ponton et al. [22]. Recently, they [23] computed accurately the screech tones from a supersonic twin-jet with Mach number 1.36.

Since it is capable to compute accurately the screech tones with CAA methods, it is desirable to apply the CAA method to study the effect of temperature on the screech tones. Therefore the main objective of this work is to study the effect of temperature on the screech tones from a supersonic round jet with a high order finite difference solver. The jet in the Mach number range from 1.10 to 1.56 is simulated in this study. Four jet reservoir temperature ratios, which are 1, 1.67, 2.32 and 2.78 respectively, are considered. The computed screech frequencies and amplitudes are compared with the experimental data by Ponton et. al. [22], and Massey et al. [14].

In the next section, the governing equations, the numerical algorithm and boundary conditions are described. Detailed numerical results and discussions are presented in section 3. Finally, a conclusion is drawn in section 4.

2 Numerical Methods

2.1 Governing Equations

To simulate the supersonic jet noise, the unsteady three dimensional compressible Favre filtered Navier-Stokes equations in Cartesian coordinates are used as the governing equations. The conservative form of the nondimensional filtered NS equations can be written as,

$$\frac{\partial q}{\partial t}+\frac{\partial}{\partial x_1}(f+f_v)+\frac{\partial}{\partial x_2}(g+g_v)+\frac{\partial}{\partial x_3}(h+h_v)=0 \tag{1}$$

where

$$q=(\bar{\rho},\bar{\rho}\tilde{u}_1,\bar{\rho}\tilde{u}_2,\bar{\rho}\tilde{u}_3,\bar{\rho}\tilde{e})^T$$

$$
f = \begin{pmatrix} \bar{\rho}\tilde{u}_1 \\ \bar{\rho}\tilde{u}_1^2 + \tilde{p} \\ \bar{\rho}\tilde{u}_1\tilde{u}_2 \\ \bar{\rho}\tilde{u}_1\tilde{u}_3 \\ (\bar{\rho}\tilde{e} + \bar{p})u_1 \end{pmatrix} \quad f_v = \begin{pmatrix} 0 \\ \tilde{\sigma}_{11} + \tau_{11} \\ \tilde{\sigma}_{12} + \tau_{12} \\ \tilde{\sigma}_{13} + \tau_{13} \\ \tilde{u_j}(\tilde{\sigma}_{1j} + \tau_{1j}) + \tilde{q}_1 + Q_1 \end{pmatrix}
$$

$$
g = \begin{pmatrix} \bar{\rho}\tilde{u}_2 \\ \bar{\rho}\tilde{u}_2\tilde{u}_1 \\ \bar{\rho}\tilde{u}_2\tilde{u}_2 + p \\ \bar{\rho}\tilde{u}_2\tilde{u}_3 \\ (\bar{\rho}\tilde{e} + \bar{p})\tilde{u}_2 \end{pmatrix} \quad g_v = \begin{pmatrix} 0 \\ \tilde{\sigma}_{12} + \tau_{12} \\ \tilde{\sigma}_{22} + \tau_{22} \\ \tilde{\sigma}_{23} + \tau_{23} \\ \tilde{u}_j(\tilde{\sigma}_{2j} + \tau_{2j}) + \tilde{q}_2 + Q_2 \end{pmatrix}
$$

$$
h = \begin{pmatrix} \bar{\rho}\tilde{u}_3 \\ \bar{\rho}\tilde{u}_3\tilde{u}_1 \\ \bar{\rho}\tilde{u}_3\tilde{u}_2 \\ \bar{\rho}\tilde{u}_3\tilde{u}_3 + \bar{p} \\ (\bar{\rho}\tilde{e} + \bar{p})\tilde{u}_3 \end{pmatrix} \quad h_v = \begin{pmatrix} 0 \\ \tilde{\sigma}_{13} + \tau_{13} \\ \tilde{\sigma}_{23} + \tau_{23} \\ \tilde{\sigma}_{33} + \tau_{33} \\ \tilde{u}_j(\tilde{\sigma}_{3j} + \tau_{3j}) + \tilde{q}_3 + Q_3 \end{pmatrix}
$$

where $\bar{\rho}$, $\tilde{u}_1$, $\tilde{u}_2$, $\tilde{u}_3$, $\bar{p}$, $\tilde{T}$ are the density, the velocities in x_1, x_2, x_3 directions, the pressure, the temperature respectively, $\tilde{e}$ is the total specific energy, and equal to $\frac{\tilde{T}}{\gamma(\gamma-1)} + \frac{1}{2}(\tilde{u}_1^2 + \tilde{u}_2^2 + \tilde{u}_3^2)$. For idea gas, $\bar{p} = \frac{\bar{\rho}\tilde{T}}{\gamma}$. The stress tensors and heat flux vector can be expressed as:

$$
\begin{aligned}
\tilde{\sigma}_{ij} &= -\tilde{\mu}\left(\frac{\partial \tilde{u}_i}{\partial x_j} + \frac{\partial \tilde{u}_j}{\partial x_i} - \frac{2}{3}\delta_{ij}\nabla \cdot \mathbf{u}\right) \\
\tilde{q}_i &= -\frac{1}{(\gamma-1)}\frac{\tilde{\mu}}{Pr}\frac{\partial \tilde{T}}{\partial x_i}
\end{aligned}
\tag{2}
$$

where $\tilde{\mu}$ is the molecular viscosity coefficient, and calculated with the Sutherland's formula. τ_{ij} and Q_i are the subgrid-scale stress and the heat flux respectively, and can be expressed as,

$$
\begin{aligned}
\tau_{ij} &= \bar{\rho}(\widetilde{u_i u_j} - \tilde{u}_i\tilde{u}_j) \\
Q_i &= \bar{\rho}(\widetilde{u_i T} - \tilde{u}_i\tilde{T})
\end{aligned}
$$

In this study, the Smagorinsky SGS model [24] is applied in LES. This method was utilized by the present authors to simulate the screech tone for twin-jet [23], and a good result was obtained.

2.2 Numerical Schemes

Numerical discretization scheme is one of the key elements of a CAA approach. In the present CAA code, the 7-point Dispersion-Relation-Preserving scheme ($\eta = 1.1$) [25] is used for spatial discretization. The 5/6-stage Low-Dissipation and Low-Dispersion Runge-Kutta (LDDRK) scheme in the 2N storage form [28] is applied for time integration. The discretization schemes have been used in our previous studies for the simulation of axisymmetric and 3D supersonic jet screech tones [20, 21].

The variable stencil Reynolds number method of Tam & Shen [29] is utilized to capture the shock in the jet core region. Differently from Tam & Shen's original method, the damping strength is determined based on a shock sensor, which was proposed by Visbal & Gaitonde [30] and Bogey et al. [31]. This method can prevent extra damping in shock-less flow region. The present authors used this method to simulate supersonic jet noise including both the screech tone [32] and broadband shock associated noise [33], and good results were obtained. The details of this method can be referred in reference [31, 32] and are not presented here for brevity.

2.3 Boundary Conditions

2.3.1 Far Field and Outflow Boundary Conditions

Boundary condition is another key element of a CAA approach. As sketched in Fig. 1 the radiation boundary condition in 3D form by Bogey & Bailly [34] suitable for weakly non-uniform mean flows is applied at the left boundary outside the nozzle and outer boundary regions where the local mean flow Mach number $M_a \leqslant 0.001$. At the downstream boundary region where $Ma \geqslant 0.001$, the outflow boundary conditions of Tam & Dong [35, 21] in 3D form are used.

2.3.2 Inflow Boundary Condition

At the nozzle exit, all nondimensional mean flow variables are given as follows:

$$\begin{aligned} \bar{\rho}_e &= \frac{\gamma(\gamma+1)\bar{p}_e}{2T_r} \\ \bar{p}_e &= \frac{1}{\gamma}\left[\frac{2+(\gamma-1)M_j^2}{\gamma+1}\right]^{\frac{\gamma}{\gamma-1}} \\ \bar{u}_e &= \left(\frac{2T_r}{\gamma+1}\right)^{\frac{1}{2}}, \qquad \bar{v}_e = 0, \qquad \bar{w}_e = 0 \end{aligned}$$

where M_j is the fully expanded Mach number of the jet, and T_r is the ratio of the jet reservoir temperature to the ambient air temperature. In this study, the under-expanded jet with Mach number M_j range from 1.2 to 1.56 is simulated, and four ratios of the jet reservoir temperature, which are 1, 1.67, 2.32 and 2.78 respectively, are computed to study the effect of temperature on the screech tones.

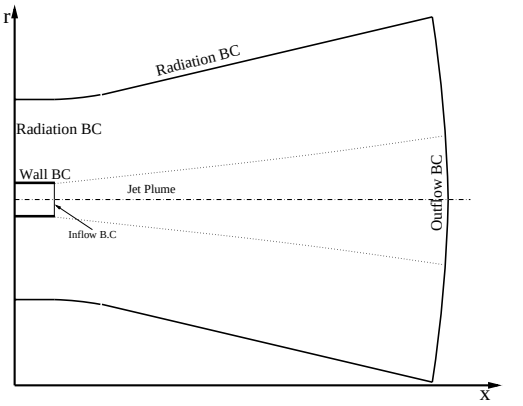

Figure 1: Boundary conditions used in the simulation.

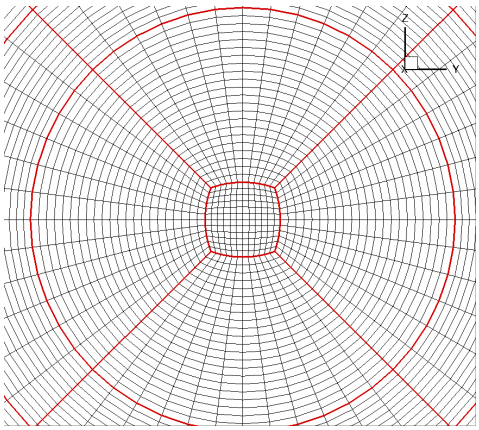

Figure 2: Cartesian mesh used in the simulation to avoid the singularity in the axis

3 Numerical Results and Discussions

In this study, the convergent nozzle with lip thickness equal to $0.2D$ is simulated, where D is the nozzle diameter in the exit plane, and equal to 1 inch. The computational domain is extended from $-5D$ to $30D$ in the x direction, and $15D$ in the radial direction. The mesh in the nozzle exist plane is shown in Fig. 2. To avoid the singularity of the mesh along the axis, the Cartesian mesh is utilized in the central of the jet, as shown in Fig. 2. The IFR method is applied on all the interior block interfaces instead of the overlap grid method. About 2.7 million grid points are used in the simulation. The CFL number in the simulation is chosen as 0.60. The final data are beginning to be exported when the simulation runs after about 30,000

time steps and any start-up transients have left the computational domain. The mean flow field is obtained after about 150,000 steps time average.

3.1 Flow Field

The instantaneous pressure fields in the $x-y$ plane from the shock containing jet with Mach number 1.4 are shown in Fig. 3. The results at four different jet reservoir temperature ratios are presented to show the effect of temperature on the pressure field. The radiated tone noise in the upstream and downstream directions can be observed clearly in each figure. This indicates screech tones are generated by the jet with high temperatures. It is shown clearly that stronger noise generated downstream for the jet with higher temperature. It can also be observed that the wavelength of the dominant screech tone decreases with the jet temperature. The instantaneous pressure fields in the nozzle exit plane ($y-z$) from the jet with Mach number 1.4 at the four jet reservoir temperature ratios are shown in Fig. 4. It is clear that the pressure pattern is anti-symmetric for the jet with reservoir temperature ratio 1.0, as shown in Fig. 4(a). This means the dominant screech mode is flapping. For the jets with higher reservoir temperature ratios as shown in Fig. 4(b), 4(c) and 4(d), the patterns are similar to be helical. A phase analysis of the screech tone is necessary to determine whether it is helical or not. The phase analysis of the noise spectra will be presented in the following section.

The time average pressure along the jet axis is plotted in Fig. 5 for the jets with $M_j = 1.2$ and 1.4 at 4 different reservoir temperatures ratios. It is clear that the jet temperature has almost no effect on the length of the shock-cells, except the strength downstream and the length of the jet core region. It is shown in Fig. 5(a) that for the jet with temperature ratio $T_r/T_\infty = 2.78$, the 8th or even the 9th shock-cell is still visible, but the 7th shock-cell is very weak and almost disappears for the jet with $T_r/T_\infty = 1.0$. It is similar for the shock-cells of the jet with $M_j = 1.4$ shown in Fig. 5(b).

3.2 Noise Spectra

The noise spectra at $r/D = 2$ in the nozzle exit plane are plotted in Fig. 6 for the jet with $M_j = 1.23$ and $T_r/T_\infty = 1.0$. The computational results are compared with the experimental data of Ponton et al. [22]. It is shown that the numerical simulation predicted correctly the frequencies and amplitudes of the dominant screech tone, as well as its two harmonics. This implies the developed CAA code for screech tone simulation is reliable. The effect of the jet temperature on the noise spectra is plotted in Fig. 7 for the jet with $M_j = 1.4$ at four different temperature ratios. The data are sampled at $r/D = 2$ in the nozzle exit plane. In each figure the frequencies and amplitudes of two dominant modes are marked. It is shown that the frequency of the first dominant mode increases with the jet temperature, but the amplitude decreases slightly. The second mode is weak in the cold jet ($Tr = 1.0$), but stronger for the hot jets. To identify the mode of the screech tone, a cross correlation is carried out for the pressure signals at two points which are located at the opposite sides of the nozzle in the exit plane. The phase difference is plotted also in Fig. 7 to determine the mode of the dominant screech tone for convenience. It is easy to find out that the pressure signals of first screech mode on the two opposite sides of the nozzle are out of phase. This indicates that the first mode is flapping. The second mode can also be identified as a flapping one. As shown previously in Fig. 4, the pressure patterns in the nozzle exit plane are similar to be helical for the hot jets with $M_j = 1.4$, except that of the cold jet. Based on the mode analysis it is not difficult to explain the pressure patterns in the nozzle exit plane. Since the amplitude of the second flapping mode (as shown in Fig. 7) in the hot jets is larger than that in the cold jet, it is coupled with the first mode, and then the helical pressure pattern is generated.

The computed frequencies of the dominant screech tones of the jet with 4 temperature ratios in the Mach number range from 1.2 to 1.56 are plotted in Fig. 8(a). Only the frequencies of the cold jet are compared with the experimental data of Ponton et al. [22], because rare reliable experimental data of screech tone of hot jet are available for comparison. It is found that the calculated frequencies of the cold jet agree well with the experimental data. The frequencies varying with the acoustic Mach number ($Ma = V_j/a_\infty$) are also plotted in Fig. 8(b), where V_j is the fully expanded velocity of the jet. It is found that for the jet with a fixed fully expanded Mach number, the non-dimensional frequency ($st = fD/a_\infty$) of the screech tone almost increases linearly with the acoustic Mach number. The computed amplitudes of the dominant screech tones varying with the Mach number M_j are plotted in Fig. 9. The data are sampled at $r/D = 2$ in the nozzle

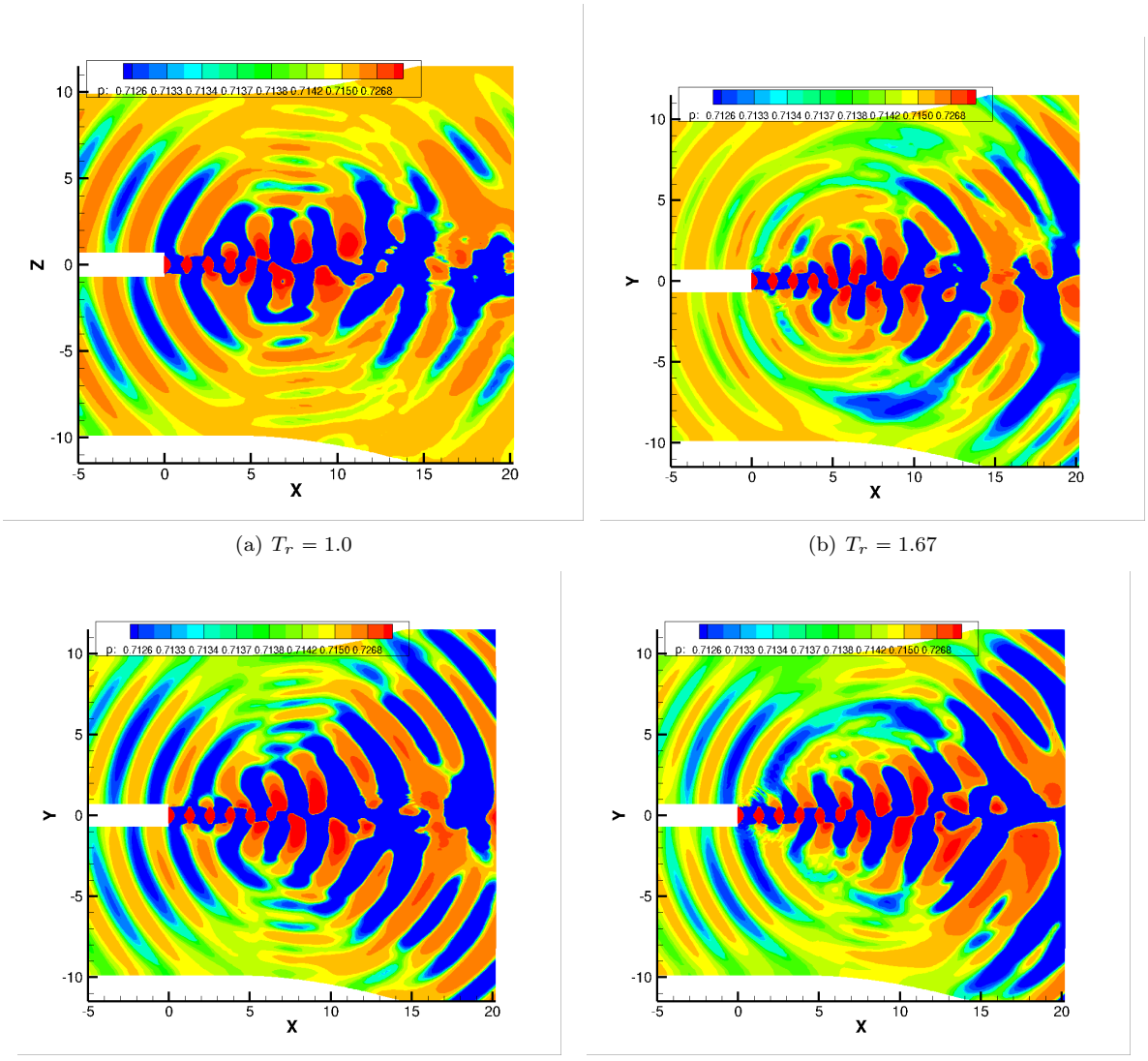

(a) $T_r = 1.0$

(b) $T_r = 1.67$

(c) $T_r = 2.32$

(d) $T_r = 2.78$

Figure 3: Instantaneous pressure fields in the $x - y$ plane for the jet with Mach number $M_j = 1.4$ at four different reservoir temperature ratios.

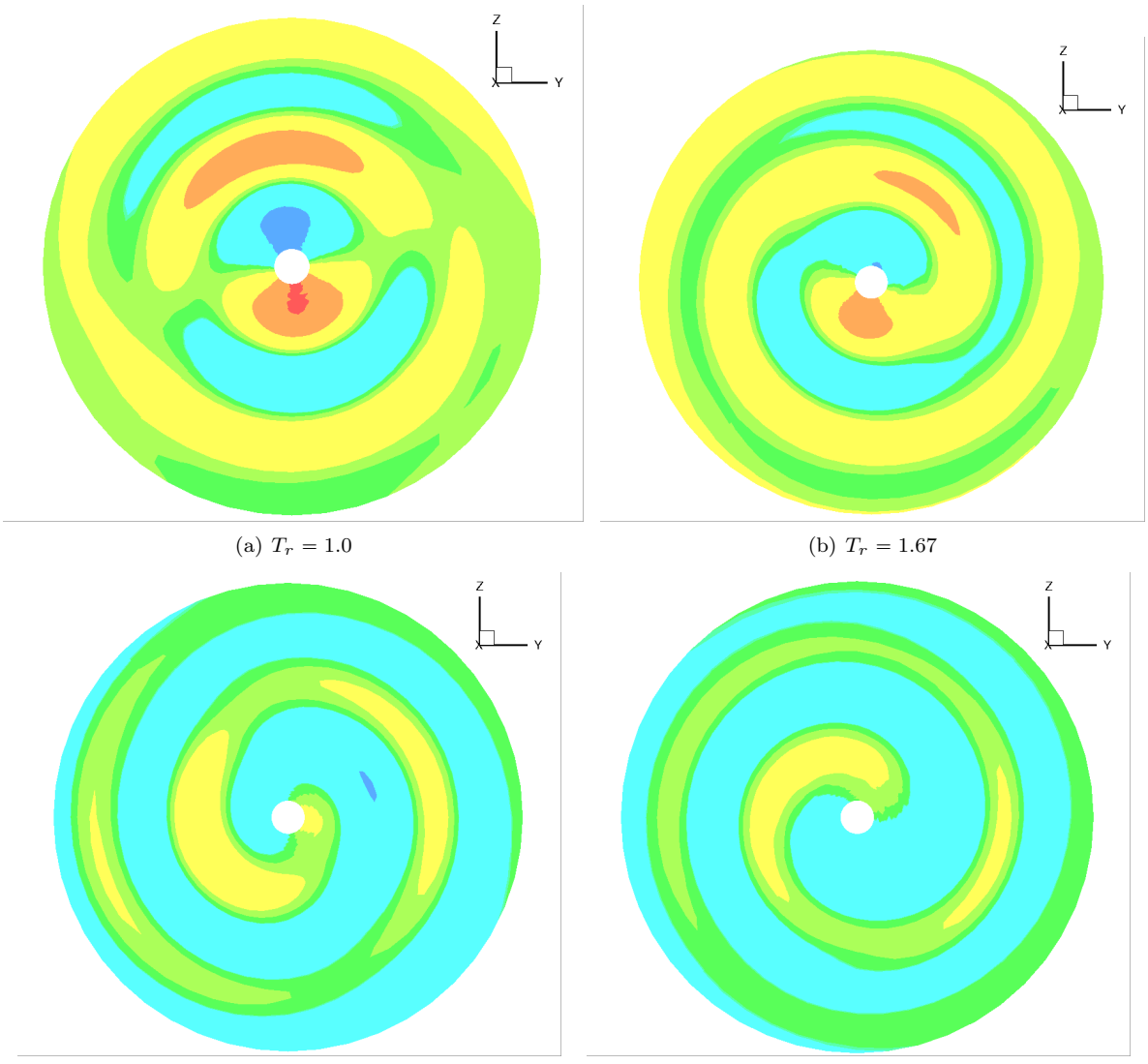

(a) $T_r = 1.0$

(b) $T_r = 1.67$

(c) $T_r = 2.32$

(d) $T_r = 2.78$

Figure 4: Instantaneous pressure field in the nozzle exit plane for the jet with Mach number $M_j = 1.4$ at four different reservoir temperature ratios.

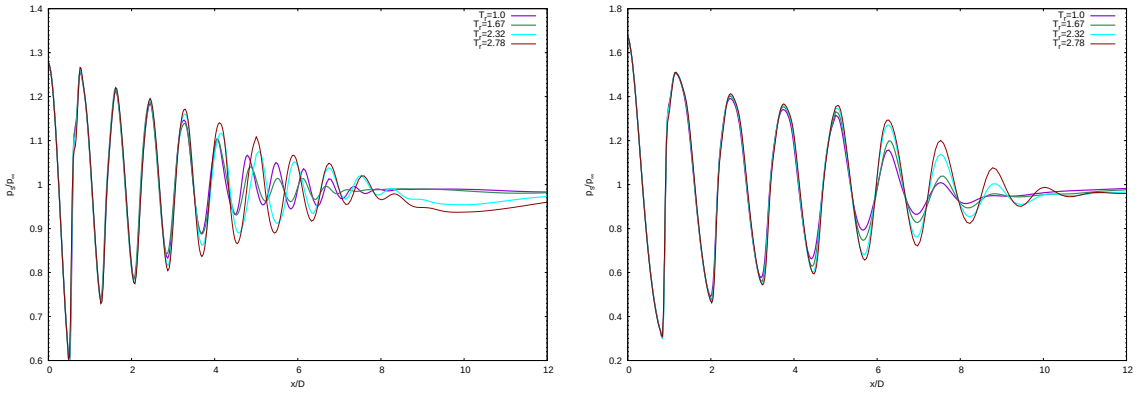

(a) $M_j = 1.20$ (b) $M_j = 1.40$

Figure 5: The pressure distribution along the axis of the jets with $M_j = 1.2$ and 1.4 at four different temperature ratios.

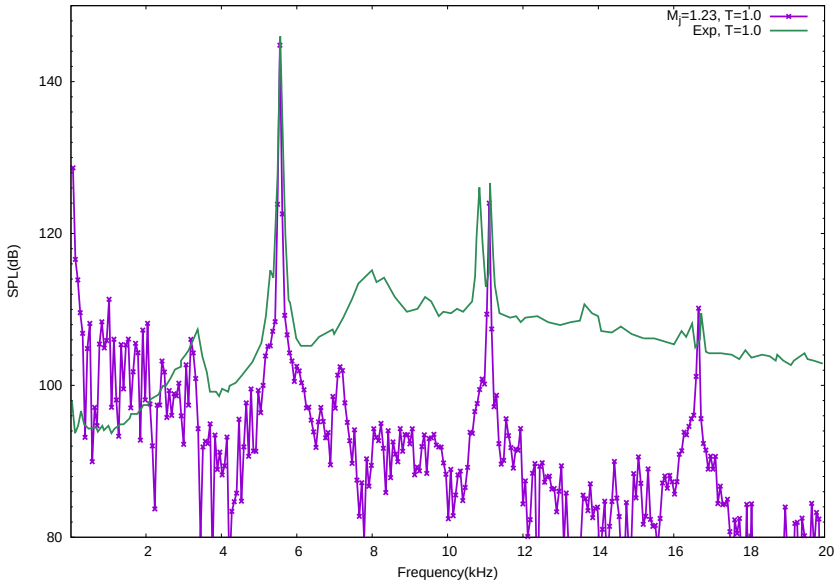

Figure 6: Noise Spectra at $r/D = 2$ in the nozzle exit plane of the jet with $M_j = 1.23$ and $T_r = 1.0$, comparing with the experimental data of Ponton et al. [22]

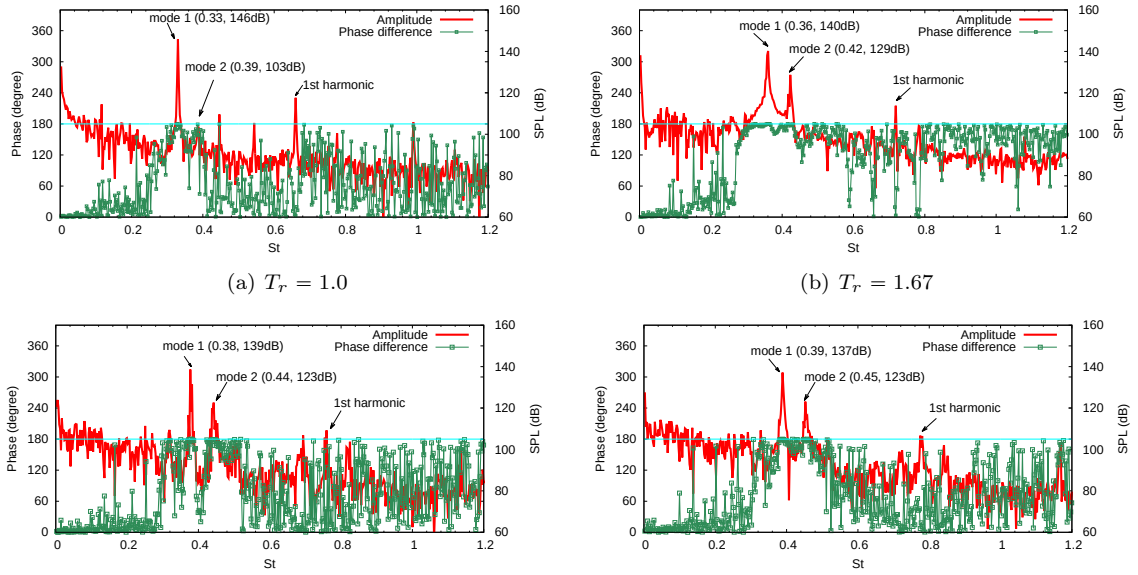

(a) $T_r = 1.0$ (b) $T_r = 1.67$

(c) $T_r = 2.32$ (d) $T_r = 2.78$

Figure 7: Noise spectra at $r/D = 2$ in the nozzle exit plane and the phase differences of the spectra of the jet with Mach number $M_j = 1.4$

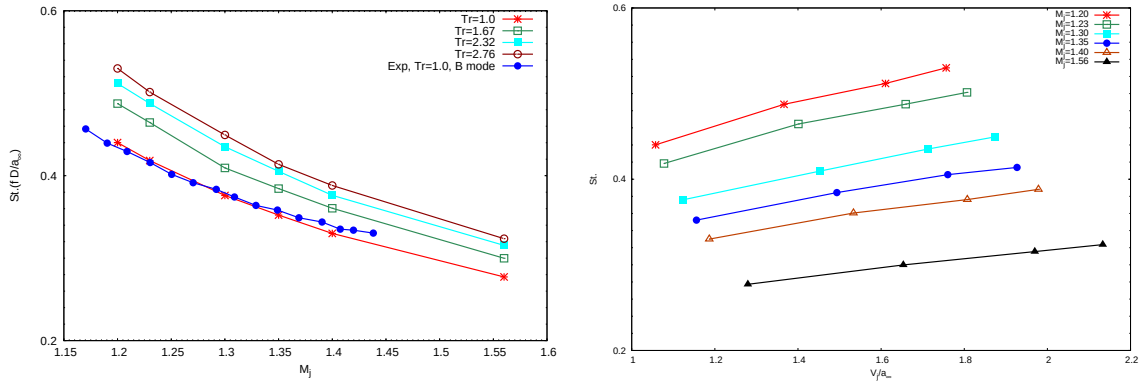

(a) (b)

Figure 8: The frequencies of the dominant screech tones ((a) varying with the fully expanded Mach number M_j, (b) varying with the acoustic Mach number $Ma = V_j/a_\infty$).

exit plane. The data of the jet at four different temperature ratios are all presented. Only the SPL of the cold jet ($Tr = 1.0$) is compared with the experimental data of Ponton et al. [22]. It is found that most of the computed amplitudes in the low Mach number range agree well with the experimental data. As shown in Fig. 9, the amplitudes of the hot screeching jets decrease slightly with the temperature. This is almost consistent with the experimental results of Massey et al. [14]. They concluded in their research that the temperature of the jet plume had little effect on the amplitude of the screech tone.

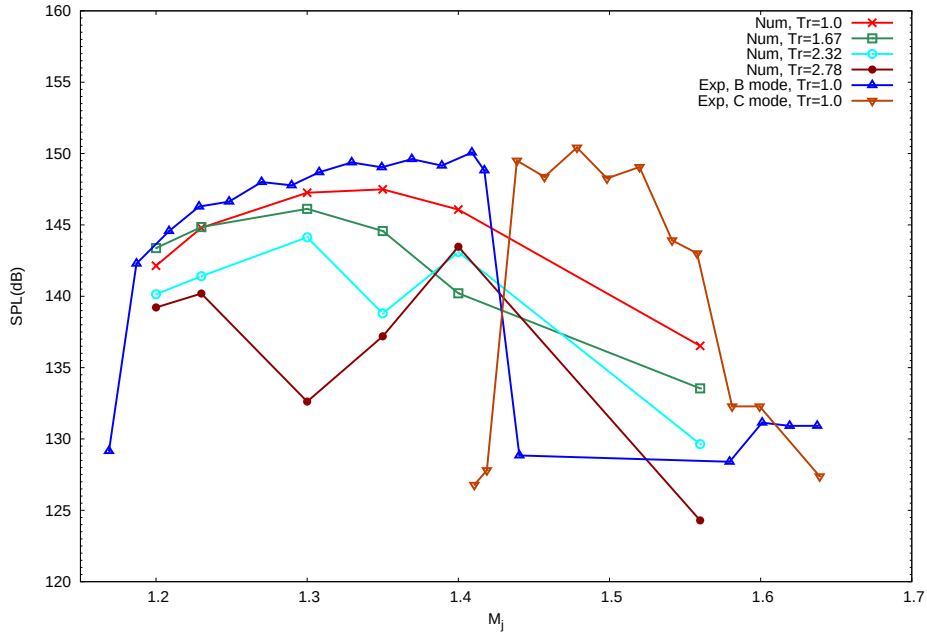

Figure 9: Amplitudes of the screech tones at $r/D = 2$ in the nozzle exit plane for the jet in the Mach number range from 1.2 to 1.56.

4 Conclusion and Future Work

In this study, the screech tones from a supersonic round jet in the Mach number range from 1.2 to 1.56 are simulated with a high order finite difference solver. Four reservoir temperature ratios, which are 1.0, 1.67, 2.32 and 2.78 respectively, are computed in the simulation for each Mach number to study the effect of temperature on the screech tone. The calculated screech frequencies and amplitudes of the cold jet ($Tr/T_\infty = 1.0$ are compared with the experimental data by Ponton et. al. [22], and a good agreement is obtained. It is found that the frequencies of the screech tones increase with the jet temperature, but the amplitudes decreases slightly with the temperature. This is consistent with the experimental results of Massey et al. [14].

A further simulation and analysis on the mechanism of the screech tone for the hot jet would be conducted in the near future. The dynamic mode decomposition would be applied to the large scale structures in the jet plume, which may be helpful in understanding the mechanism of screech tone of the hot jet.

References

[1] A. Powell. On the noise emanating from a two-dimensional jet above the critical pressure. *Aeronautical Quarterly*, 4:103–122, 1953.

[2] G. Raman. Supersonic jet screech: Half-century from Powell to the present. *Journal of Sound and Vibration*, 225(3):543–571, 1999.

[3] M. Merle. Sur la fre'quencies des sondes e'mises par un jet d'air 'agrand vitesse. *C. R. Academy of Science Paris*, 243:490–493, 1956.

[4] M. G. Davies and D. E. S. Oldfield. Tones from a choked axisymmetric jet. *Acoustica*, 12(4):257–277, 1962.
[5] R. Westley and J.H. Woolley. An investigation of the near noise field of a choked axisymmetric air jet. Technical report, National Research Council of Canada, National Aeronautical Establishment, Aeronautical Report LR-506, June, 1968.
[6] L. J. Poldervaart, A. P. Wijnands, and L. Bronkhurst. Aerosonic games with the aid of control elements and externally generated pulses. Number 20, pages AGARD CP–131 1–4, 1973.
[7] Y. Y. Chan. A simple model of shock-cell noise generation and its reduction. page NRC/NAE (Canada) Aero. Report LR 564, 1972.
[8] M. K. Ponton and J. M. Seiner. The effects of nozzle exit lip thickness on plume resonance. *Journal of Sound and Vibration*, 154(3):531–549, 1992.
[9] J. Panda. Shock oscillation in underexpanded screeching jets. *Journal of Fluid Mechanics*, 363:173–198, 1998.
[10] J. Panda and R. G. Seasholtz. Measurement of shock structure and shock-vortex interaction in underexpanded jets using rayleigh scattering. *Physics of Fluids*, 11(12):3761–3777, 1999.
[11] C. K. W. Tam, J. A. Jackson, and J. M. Seiner. A multiple-scales model of shock-cell structure of imperfectly expanded supersonic jets. *Journal of Fluid Mechanics*, 153:123–149, 1985.
[12] P. J. Morris, T. R. S. Bhat, and G. Chen. A linear shock-cell model for jets of arbitrary exit geometry. *Journal of Sound Vibration*, 132:199–211, 1989.
[13] C. K. W. Tam, J. M. Seiner, and J. C. Yu. Proposed relationship between broadband shock associated noise and screech tones. *Journal of Sound and Vibration*, 110:309–321, 1986.
[14] K. C. Massey, K. K. Ahuja, R. R. Jones, and C. K. W. Tam. Screech tones of supersonic heated free jets. In *AIAA Paper 1994–0141*, 1994.
[15] K. C. Massey, K. K. Ahuja, and N. Messersmith. Forward flight effects on heated and unheated rectangular jets. In *AIAA Paper 2002-2483*, 2002.
[16] K. C. Massey, K. K. Ahuja, and R. Gaeta. Noise scaling for unheated rectangular jets. In *AIAA Paper 2004-2946*, 2004.
[17] H. Shen and C. K. W. Tam. Numerical simulation of the generation of axisymmetric mode jet screech tones. *AIAA Journal*, 36(10):1801–1807, 1998.
[18] H. Shen and C. K. W. Tam. Three-dimensional numerical simulation of the jet screech phenomenon. *AIAA Journal*, 40(1):33–41, 2002.
[19] H. Shen and C. K. W. Tam. The effects of jet temperature and nozzle lip thickness on screech tones. pages AIAA Paper 1999–1860, 1999.
[20] X. D. Li and J. H. Gao. Numerical simulation of the generation mechanism of axisymmetric supersonic jet screech tones. *Physics of Fluids*, 17:085105, 2005.
[21] X. D. Li and J. H. Gao. Numerical simulation of the three dimensional screech phenomenon from a circular jet. *Physics of Fluids*, 20:035101, 2008.
[22] Michael K. Ponton, John M. Seiner, and M. C. Brown. Near field pressure fluctuations in the exit plane of a choked axisymmetric nozzle. NASA Technical Memorandum 113137, Langley Research Center, November 1997.
[23] J. H. Gao, X. Xu, and X. D. Li. Numerical simulation of supersonic twin-jet noise with high-order finite difference scheme. *AIAA Journal*, 56(1):290–300, 2018.
[24] J. S. Smagorinsky. General circulation experiments with the primitive equations. *Mothly Weather Review*, 91(3):99–165, 1963.
[25] C. K. W. Tam and J. C. Webb. Dispersion-relation-preserving finite difference schemes for computational acoustics. *Journal of Computational Physics*, 107:262–281, 1993.
[26] J. H. Gao. A block interface flux reconstruction method for numerical simulation with high order finite difference schemes. *Journal of Computational Physics*, 241:1–17, 2013.
[27] J. H. Gao and X. D. Li. Improved grid block interface flux reconstruction method for high order finite difference scheme. *AIAA Journal*, 53(7):1761–1773, 2015.
[28] D. Stanescu and W. G. Habashi. 2n-storage low-dissipation and low-dispersion runge-kutta schemes for computational aeroacoustics. *Journal of Computational Physics*, 143(2):674–681, 1998.
[29] C. K. W. Tam and H. Shen. Direct Computation of nonlinear acoustic pulses using high order finite difference schemes. pages AIAA Paper 1993–4325, 1993.

[30] M. R. Visbal and D. V. Gaitonde. Shock capturing using compact-differencing-based methods. pages AIAA 2005–1265, 2005.

[31] C. Bogey, N. Cacqueray, and C. Bailly. A shock-capturing methodology based on adaptative spatial filtering for high-order non-linear computations. *Journal of Computational Physics*, 228:1447–1465, 2009.

[32] J. H. Gao and X. D. Li. Large eddy simulation of supersonic jet noise from a circular nozzle. *International Journal of Aeroacoustics*, 10(4):465–474, 2011.

[33] J.H. Gao and X.D. Li. Numerical simulation of broadband shock-associated noise from a circular supersonic jet. pages AIAA Paper 2010–0275. 48th AIAA Aerospace Sciences Meeting, 2010.

[34] C. Bogey and C. Bailly. Three-dimensional non-reflective boundary conditions for acoustic simulations: Far field formulation and validation test cases. *ACTA Acustica United With Acustica*, 88:463–471, 2002.

[35] C. K. W. Tam and Z. Dong. Radiation and outflow boundary conditions for direct computation of acoustic and flow disturbances in a nonuniform mean flow. *Journal of Computational Acoustics*, 4:175–201, 1996.